Regulation of Cytokine Receptors by Golgi N-Glycan Processing and Endocytosis

Emily A. Partridge, *et al.*

Science **306**, 120 (2004);
DOI: 10.1126/science.1102109

inhibitor of ubiquitin-dependent degradation in multiple experimental settings.

The specificity of ubistatin A for K48-linked ubiquitin chains suggested that it might bind at the Ub-Ub interface, which is well defined in K48-linked chains but is not present in K63-linked di-ubiquitin (Ub_2) (*22*). We performed nuclear magnetic resonance (NMR) titration studies of K48-linked Ub_2 by using a segmental labeling strategy (*23*). Well-defined site-specific perturbations were observed in the resonances of the backbone amides of both Ub units in Ub_2 (Fig. 3), indicating that the hydrophobic patch residues L8, I44, V70 (*24*), and neighboring sites (including basic residues K6, K11, R42, H68, and R72) experienced alterations in their molecular environment upon binding of ubistatin A. The same hydrophobic patch is involved in the formation of the interdomain interface in Ub_2 (*23*, *25*) and mediates the binding of ubiquitin to multiple proteins containing CUE (coupling of ubiquitin conjugation to ER degradation), UBA, and UIM domains (*17*). At the high concentrations of compound used in the NMR titration experiments, ubistatin A induced a similar pattern of chemical shift perturbations in monomeric ubiquitin, suggesting that the effect of ubistatin A on Ub_2 arises from its direct binding to the hydrophobic patch and the basic residues around it. The same sites are perturbed when ubistatin A binds tetra-Ub chains (*26*).

Although there is intense interest in developing drugs for defined molecular targets, it is often difficult to know a priori which proteins can be most effectively targeted with small molecules. Our study demonstrates that chemical genetic screens in complex biochemical systems such as *Xenopus* extracts can identify small-molecule inhibitors that act through unexpected mechanisms. Although target identification remains challenging, our work highlights the value of reconstituted biochemical systems to illuminate the mechanism of action of inhibitors discovered in unbiased screens. The recent approval of the 20S proteasome inhibitor Velcade (Millenium Pharmaceuticals, Cambridge, MA) for treatment of relapsed multiple myeloma (*27*) has suggested that the ubiquitin-proteasome system is an attractive target for cancer drug development. The identification of ubistatins indicates that the ubiquitin chain itself provides another potential opportunity for pharmacological intervention in this important pathway.

References and Notes

1. T. U. Mayer, *Trends Cell Biol.* **13**, 270 (2003).
2. J. M. Peters, *Mol. Cell* **9**, 931 (2002).
3. Materials and methods are available as supporting material on *Science* Online.
4. M. Dasso, J. W. Newport, *Cell* **61**, 811 (1990).
5. J. Minshull, H. Sun, N. K. Tonks, A. W. Murray, *Cell* **79**, 475 (1994).
6. L. A. Walling, N. R. Peters, E. J. Horn, R. W. King, *J. Cell. Biochem.* **S37**, 7 (2001).
7. C. M. Pfleger, M. W. Kirschner, *Genes Dev.* **14**, 655 (2000).
8. A. Salic, E. Lee, L. Mayer, M. W. Kirschner, *Mol. Cell* **5**, 523 (2000).
9. N. Peters, R. W. King, unpublished data.
10. R. Verma, H. McDonald, J. R. Yates 3rd, R. J. Deshaies, *Mol. Cell* **8**, 439 (2001).
11. D. Skowyra *et al.*, *Science* **284**, 662 (1999).
12. J. H. Seol *et al.*, *Genes Dev.* **13**, 1614 (1999).
13. R. Verma, R. Oania, J. Graumann, R. J. Deshaies, *Cell* **118**, 99 (2004).
14. R. Verma *et al.*, *Science* **298**, 611 (2002); published online 15 August 2002; 10.1126/science.1075898.
15. T. Yao, R. E. Cohen, *Nature* **419**, 403 (2002).
16. L. Meng *et al.*, *Proc. Natl. Acad. Sci. U.S.A.* **96**, 10403 (1999).
17. R. Hartmann-Petersen, M. Seeger, C. Gordon, *Trends Biochem. Sci.* **28**, 26 (2003).
18. J. Peng *et al.*, *Nat. Biotechnol.* **21**, 921 (2003).
19. C. M. Pickart, *Cell* **116**, 181 (2004).
20. M. Zhang, C. M. Pickart, P. Coffino, *EMBO J.* **22**, 1488 (2003).
21. K. M. Sakamoto *et al.*, *Mol. Cell. Proteomics* **2**, 1350 (2003).
22. R. Varadan *et al.*, *J. Biol. Chem.* **279**, 7055 (2004).
23. R. Varadan, O. Walker, C. Pickart, D. Fushman, *J. Mol. Biol.* **324**, 637 (2002).
24. Single-letter abbreviations for the amino acid residues are as follows: H, His; I, Ile; K, Lys; L, Leu; R, Arg; and V, Val.
25. W. J. Cook, L. C. Jeffrey, M. Carson, Z. Chen, C. M. Pickart, *J. Biol. Chem.* **267**, 16467 (1992).
26. D. Fushman, unpublished data.
27. J. Adams, *Nat. Rev. Cancer* **4**, 349 (2004).
28. R. Verma *et al.*, *Mol. Biol. Cell* **11**, 3425 (2000).

29. We thank the Developmental Therapeutics Program, National Cancer Institute, for providing access to compound collections, C. Pickart for tetraubiquitin chains of defined linkages, A. Salic for recombinant Axin and β-catenin-luciferase, and C. Sawyers for AR-GFP. G.T. is supported by NIH National Research Service Award GM068276. K.M.S. is supported by a UCLA Specialized Programs of Research Excellence in Prostate Cancer Development Research Seed Grant (P50 CA92131), U.S. Department of Defense (DAMD17-03-1-0220), and NIH (R21CA108545). P.C. is supported by NIH R01 GM-45335. D.F. is supported by NIH grant GM65334. R.J.D. is supported by HHMI and the Susan G. Komen Breast Cancer Foundation (DISS0201703). R.W.K. is supported by the NIH (CA78048 and GM66492), the McKenzie Family Foundation, and the Harvard-Armenise Foundation and is a Damon Runyon Scholar. Screening facilities at the Harvard Institute of Chemistry and Cell Biology were supported by grants from the Keck Foundation, Merck and Company, and Merck KGaA. R.J.D. is a founder and paid consultant of Proteolix, which is negotiating with Caltech and Harvard to license a patent related to ubistatin. Molecular interaction data have been deposited in the Biomolecular Interaction Network Database with accession codes 151787 to 151791.

Supporting Online Material

www.sciencemag.org/cgi/content/full/306/5693/117/DC1
Materials and Methods
Figs. S1 to S8
Table S1

1 June 2004; accepted 6 August 2004

Regulation of Cytokine Receptors by Golgi N-Glycan Processing and Endocytosis

Emily A. Partridge,[1,3] Christine Le Roy,[1] Gianni M. Di Guglielmo,[1] Judy Pawling,[1] Pam Cheung,[1,2] Maria Granovsky,[1,2] Ivan R. Nabi,[4] Jeffrey L. Wrana,[1,2] James W. Dennis[1,2,3]*

The Golgi enzyme β1,6 N-acetylglucosaminyltransferase V (Mgat5) is upregulated in carcinomas and promotes the substitution of N-glycan with poly N-acetyllactosamine, the preferred ligand for galectin-3 (Gal-3). Here, we report that expression of Mgat5 sensitized mouse cells to multiple cytokines. Gal-3 cross-linked Mgat5-modified N-glycans on epidermal growth factor and transforming growth factor–β receptors at the cell surface and delayed their removal by constitutive endocytosis. Mgat5 expression in mammary carcinoma was rate limiting for cytokine signaling and consequently for epithelial-mesenchymal transition, cell motility, and tumor metastasis. Mgat5 also promoted cytokine-mediated leukocyte signaling, phagocytosis, and extravasation in vivo. Thus, conditional regulation of N-glycan processing drives synchronous modification of cytokine receptors, which balances their surface retention against loss via endocytosis.

Co-translational modification of proteins in the endoplasmic reticulum by N-glycosylation facilitates their folding and is essential in single-cell eukaryotes. Metazoans have additional Golgi enzymes that trim and remodel the N-glycans, producing complex-type N-glycans on glycoproteins destined for the cell surface. Mammalian development requires complex-type N-glycans containing N-acetyllactosamine antennae, because their complete absence in Mgat1-deficient embryos is lethal (*1*, *2*). Deficiencies in N-acetylglucosaminyltransferase II and V (Mgat2 and Mgat5) acting downstream of Mgat1 reduce the content of N-acetyllactosamine, and mutations in these loci result in viable mice with a number of tissue defects (*3*, *4*). N-glycan processing generates ligands for various mammalian lectins, but the consequences of these interactions are poorly understood. The galectin family of N-acetyllactosamine-binding lectins has been implicated in cell

growth, endothelial cell morphogenesis, angiogenesis (*5*), cell adhesion (*6*), and cancer metastasis (*7*). Galectins are expressed widely in metazoan tissues, located in the cytosol and nucleus, and secreted by a nonclassical pathway to the cell surface (*8*).

Galectin-3 (Gal-3) binds to poly-N-acetyllactosamine (i.e., a polymer of Galβ1,4GlcNAcβ1,3) with higher affinity than to the more ubiquitous N-acetyllactosamine antennae (*9*), and Mgat5 controls production of these larger polymers by producing the preferred intermediate for their addition (fig. S1A) (*10*). The nonlectin N-terminal domain of Gal-3 mediates pentamer formation in the presence of multivalent ligands, thereby cross-linking glycoproteins in proportion to ligand concentrations (*11*). The resulting superstructure of galectins and glycoproteins at the cell surface generates a molecular lattice. Mgat5-modified N-glycans on T cell receptors bind Gal-3, which opposes antigen-dependent clustering and suppresses autoimmune disease (*12*). Here, we examine the possibility that Mgat5-modified N-glycans on cytokine receptors oppose constitutive endocytosis by retaining surface receptors where membrane remodeling is active, notably in tumor cells and monocytes (model in fig. S1B).

The Mgat5-deficient background suppresses the oncogenic potency of a polyomavirus middle T oncogene (PyMT) transgene in mice (*4*). The PyMT protein is a cytosolic scaffold that promotes Src, phosphatidylinositol (PI) 3-kinase, and Shc/Ras activation (*13*), but activation of these intracellular pathways remains partially dependent on host cell responses to extracellular stimuli and to Mgat5-modified N-

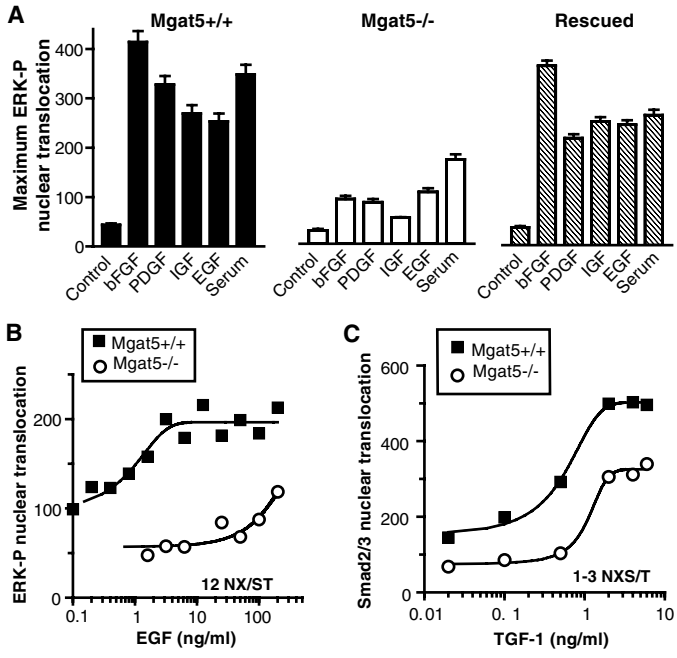

Fig. 1. Mgat5-modified N-glycans promote cytokine signaling. (**A**) Nuclear translocation of Erk-P 10 min after stimulation with cytokines (100 ng/ml) or 5% fetal calf serum, measured by scan array immunofluorescence imaging (ArrayScan, Cellomics, Incorporated, Pittsburgh, PA). (**B**) Erk-P nuclear translocation 10 min after stimulation with EGF. (**C**) Smad2 and 3 nuclear translocation 45 min after stimulation with TGF-β1.

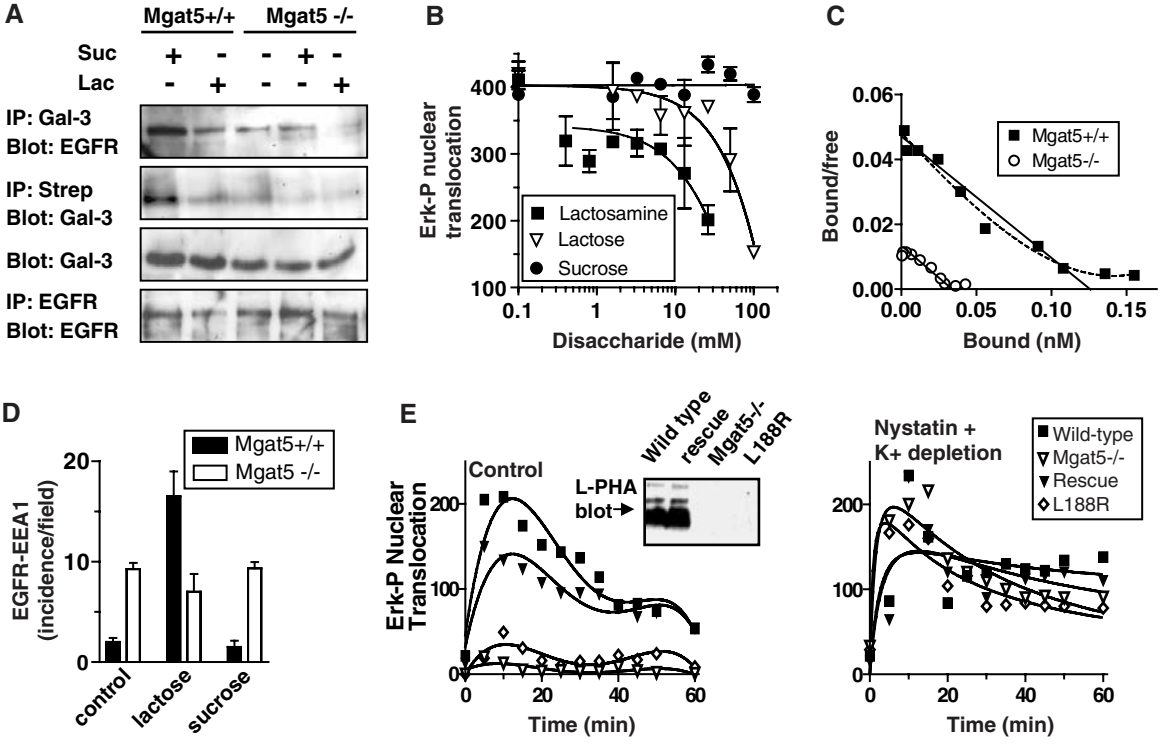

Fig. 2. Cell-surface EGFR binds to Gal-3 in an Mgat5-dependent manner. (**A**) Mgat5$^{+/+}$ and Mgat5$^{-/-}$ cells were pretreated as indicated, then subjected to DTSSP (dithio-bis-suffosuccinimydyl propionate) cross-linking and biotinylation of surface proteins. Biotinylated proteins were captured on streptoavidin-agarose beads. Sucrose and untreated cells were identical, and data shown are representative of three independent experiments. (**B**) EGF stimulated Erk-P nuclear translocation after a 24-hour pretreatment with lactose, N-acetyllactosamine, or sucrose in Mgat5$^{+/+}$ cells. (**C**) Scatchard plot of EGFR ^{125}I-EGF binding to Mgat5$^{+/+}$ and Mgat5$^{-/-}$ cells revealed 14,000 and 2500 binding sites per cell, with affinities of 2.7 and 2.5 nM, respectively. (**D**) Co-localization of EGFR with the endosome protein EEA-1 by immunofluorescence. (**E**) Erk-P nuclear translocation in cells pretreated with buffer (left) or nystatin plus K$^+$ depletion (right) before addition of EGF (100 ng/ml). Mgat5$^{-/-}$ cells were infected with retrovirus vectors for expression of either Mgat5 (rescued) or a mutant form of Mgat5 (L188R). (Inset) A blot of cell lysates probed with L-PHA lectin to reveal Mgat5-modified N-glycans.

[1]Samuel Lunenfeld Research Institute, Mount Sinai Hospital, 600 University Avenue, Toronto, ON M5G 1X5, Canada. [2]Department of Medical Genetics and Microbiology, University of Toronto, Toronto, ON M5S 1A8, Canada. [3]Department of Laboratory Medicine and Pathology, [4]Department of Anatomy, Cell Biology, and Physiology, University of British Columbia, Vancouver, BC V6T 1Z3, Canada.

*To whom correspondence should be addressed. E-mail: Dennis@mshri.on.ca

glycans (*4*). To explore this interaction, we isolated mammary epithelial tumor cells lines from PyMT transgenic mice on Mgat5$^{-/-}$ and Mgat5$^{+/+}$backgrounds and compared their responsiveness to growth factors by measuring phosphorylation and nuclear translocation of extracellular signal–regulated kinase (Erk) (Fig. 1A and fig. S2). Mgat5$^{-/-}$ tumor cells were less responsive than Mgat5$^{+/+}$ cells to epidermal growth factor (EGF), insulin-like growth factor (IGF), platelet-derived growth factor (PDGF), basic fibroblast growth factor (bFGF), and fetal calf serum, but infection of the cells with a retroviral vector encoding Mgat5 restored responsiveness (Fig. 1B and fig. S3). These cytokine receptors are all highly N-glycosylated with 8 to 16 N-glycosylation sites (N-X-S/T). Characterization of EGF receptors (EGFR) in carcinoma cells has revealed 10 to 12 occupied sites, and a subset of the N-glycans are Mgat5-modified and extended with poly-N-acetyllactosamine (*14*). The transforming growth factor–β (TGF-β) receptors TβRI and TβRII have only one and three N-X-S/T consensus sites, respectively. Mgat5$^{-/-}$ cells displayed a two- to threefold decrease in sensitivity to TGF-β compared with the ~100-fold decrease in sensitivity to EGF, PDGF, IGF-1, and FGF, supporting the notion that both Golgi processing (i.e., Mgat5 and poly-N-acetyllactosamine) and the number of N-glycans per receptor are important (Fig. 1, B and C, and fig. S3).

Next we probed the cell surface with a chemical cross-linker, which revealed that EGFR was associated with Gal-3 on the surface of Mgat5$^{+/+}$ cells whereas this interaction was greatly reduced on Mgat5$^{-/-}$ cells (Fig. 2A). Pretreatment of Mgat5$^{+/+}$ tumor cells with lactose, a competitive inhibitor of Gal-3 binding, blocked EGFR–Gal-3 cross-linking, confirming that the carbohydrate-reactive domain of Gal-3 is required. Lactose pretreatment also depleted surface Gal-3 on Mgat5$^{+/+}$ cells, producing a phenocopy of the Mgat5$^{-/-}$ cells. Furthermore, lactose and, with greater effect, N-acetyllactosamine dampened EGF-dependent activation of Erk in Mgat5$^{+/+}$ cells (Fig. 2B). Thus, surface residency of both Gal-3 and glycoprotein receptors displays a dependency on Mgat5 modification of the receptor N-glycans.

Receptor density at the cell surface is influenced by rates of de novo production, endocytosis, recycling, and degradation (*15*). Scatchard analysis revealed sixfold fewer EGFRs at the cell surface in mutant cells (Fig. 2C), although total EGFR amounts were not different between Mgat5$^{+/+}$ and Mgat5$^{-/-}$ cell lysates (Fig. 2A). The affinity of EGF binding (2 to 3 nM) was the same in Mgat5$^{+/+}$ and Mgat5$^{-/-}$ cells, consistent with previous observations that ligand affinity is not markedly altered by variations in N-glycan processing (*16*). Mgat5$^{-/-}$ cells displayed fourfold greater co-localization of EGFR with EEA-1, an early endosomal marker (Fig. 2D and fig. S6A). Pretreatment of Mgat5$^{+/+}$ cells with lactose but not sucrose promoted receptor accumulation in the endosomes, mimicking the distribution observed in untreated Mgat5$^{-/-}$ cells and providing further evidence that receptors are anchored at the cell surface by the lattice. In the absence of the lattice, receptor amounts increase in the early endosomes, possibly because of reduced trafficking downstream of receptor tyrosine kinase signaling (*17*). Lastly, the Mgat5$^{-/-}$ signaling deficiency could be rescued by K^+ depletion and nystatin treatment, agents that inhibit endocytosis (Fig. 2E and figs. S2C and S4). This chemical rescue of signaling was comparable to a genetic rescue using Mgat5, whereas a mutated Mgat5 [Lys^{188} → Arg^{188} (L188R)] that could not enter the Golgi failed to rescue signaling (Fig. 2E).

Ligand binding and autophosphorylation of EGFR stimulates clathrin-dependent EGFR endocytosis, where signaling is briefly amplified and then followed by transit of receptors

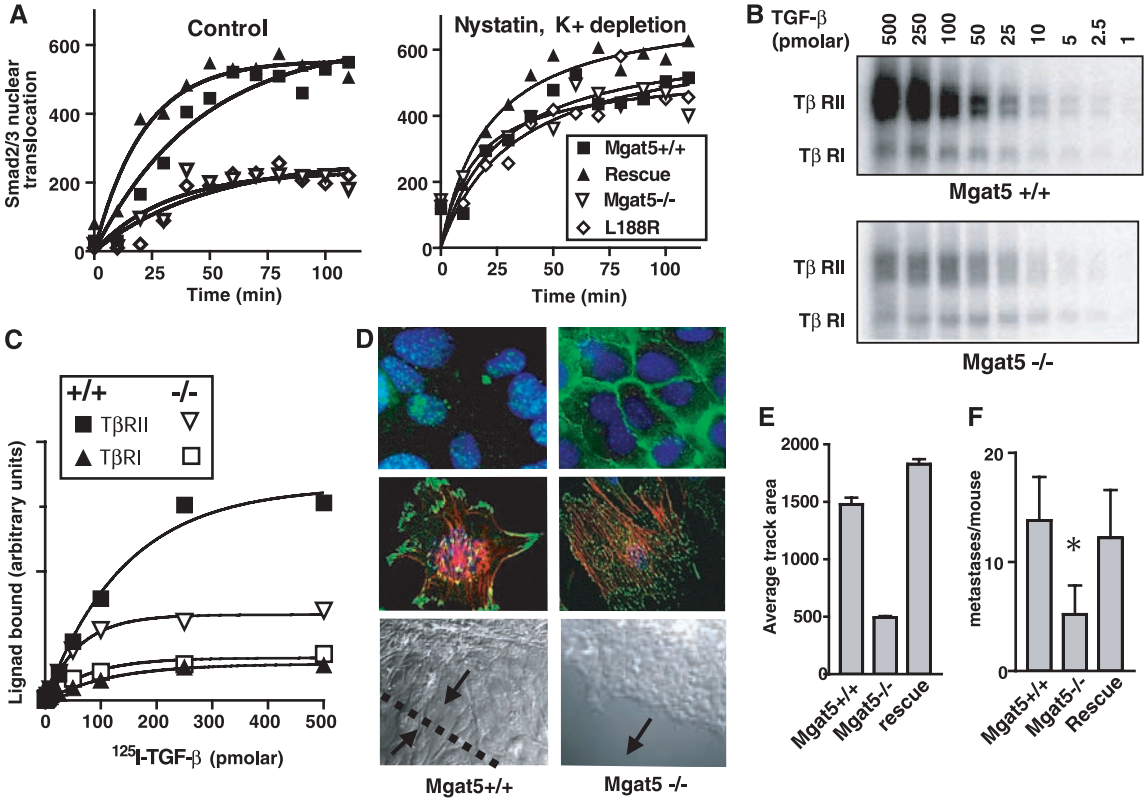

Fig. 3. EMT and the malignant phenotype are dependent on Mgat5. (**A**) Smad2 and 3 nuclear translocation in cells pretreated with buffer (left) or nystatin plus K^+ depletion (right) before addition of TGF-β (5 ng/ml). Mgat5$^{+/+}$, Mgat5$^{-/-}$, and mutant cells were infected with Mgat5 retroviral vectors. (**B**) Autoradiograph showing ^{125}I-TGF-β1 binding to cell-surface TβR. The identities of TβRI and TβRII were confirmed by immunoprecipitation. (**C**) ^{125}I-TGF-β1 bound to TGF-β receptors was quantified by densitometry. (**D**) E-cadherin (green) in tight junctions of Mgat5$^{+/+}$ and Mgat5$^{-/-}$ tumor cell monolayers revealed by immunofluorescence. Nuclear DNA is revealed by Hoechst staining. Cells plated at low density in second row are stained for actin microfilaments with rhodamine-phalloidin (red) and antibodies against vinculin (green). In the third row, contact inhibition is assessed by scratch-wounding confluent cell monolayers. The arrow indicates direction of cell movement, showing closure of the wound at 24 hours by Mgat5$^{+/+}$ but not by Mgat5$^{-/-}$ cells. (**E**) Cell motility on fibronectin-coated wells measured by scan array microbead clearance over 18 hours and expressed as mean ± SE for 100 cell tracks. (**F**) Spontaneous lung metastases (mean ± SE, $n = 6$) in wild-type mice (*$P < 0.01$).

to recycling or proteolytic compartments (*18*). In contrast, TβRII internalization is ligand-independent and occurs via both clathrin- and caveolae-dependent pathways (*19*). In spite of the differences between TβR and EGFR receptor dynamics, their regulation by the lattice was qualitatively similar. TβRII receptors associate with Gal-3 in an Mgat5-dependent manner, and the interaction could be blocked by lactose (fig. S6A). TGF-β signaling in mutant cells was restored by infection with the Mgat5 retroviral vector and by blocking endocytosis with the use of K^+ depletion and nystatin (Fig. 3A and fig. S5B). Total TβRII amounts were similar in mutant and wild-type cells, but more were localized to endosomes and less were at the surface in mutant cells (figs. S5C and S6B). Binding of ^{125}I-labeled TGF-β1 to surface TβRII was reduced 2.3-fold, whereas binding to TβRI was unchanged, an effect consistent with the number of N-X-S/T sites per receptor (i.e., three and one, respectively) (Fig. 3, B and C). We conclude that cytokine receptors are cleared from the surface of Mgat5$^{-/-}$ cells more rapidly but are delayed in the early endosomes compared to Mgat5^{++} cells.

Epithelial-mesenchymal transition (EMT) in epithelial cancers is characterized by the loss of adhesion junctions, increased membrane remodeling, and metastasis (*20*). The Mgat5$^{+/+}$ tumor cells displayed EMT with loss-of-adhesion junctions, a fibroblastic morphology with lamelipodia containing active signaling, and reduced contact inhibition in a scratch-wound assay (Fig. 3D). In contrast, Mgat5$^{-/-}$ tumor cells retained an epithelial morphology characterized by E-cadherin localization in cell adhesion junctions, cortical actin stress fibers, small focal adhesions, and strong contact inhibition of growth. EMT could be induced in Mgat5$^{-/-}$ by infecting the cells with a retroviral vector for expression of Mgat5. In vitro, wild-type and Mgat5-rescued mutant cells displayed greater cell motility (Fig. 3E), and in vivo these cells produced significantly greater numbers of lung tumor metastases, than Mgat5$^{-/-}$ cells (Fig. 3F). We conclude that Mgat5 is necessary for EMT and supplies positive feedback through cytokine receptors to Ras, PI3 kinase, and Smad2 and 3 signaling (*20*). The Ras-Raf-Ets pathway positively regulates Mgat5 transcription (*21*). TGF-β signaling also stimulates Mgat5 expression in mesenchymal cells (*22*), and we confirmed that TGF-β increased the surface expression of Mgat5-modified N-glycans (fig. S5E). TGF-β induces its own gene expression as well as that of other cytokines, and, cumulatively, these sources of positive feedback appear to maintain the EMT-invasive phenotype. Suppressors of constitutive endocytosis other than the lattice described here may promote tumor progression. In this regard, the metastasis suppressor protein Nm23-H1 is a nucleotide diphosphate kinase that supplies guanine triphosphate (GTP) to the small guanine triphosphatase (GTPase) dynamin required for membrane invagination (*23*).

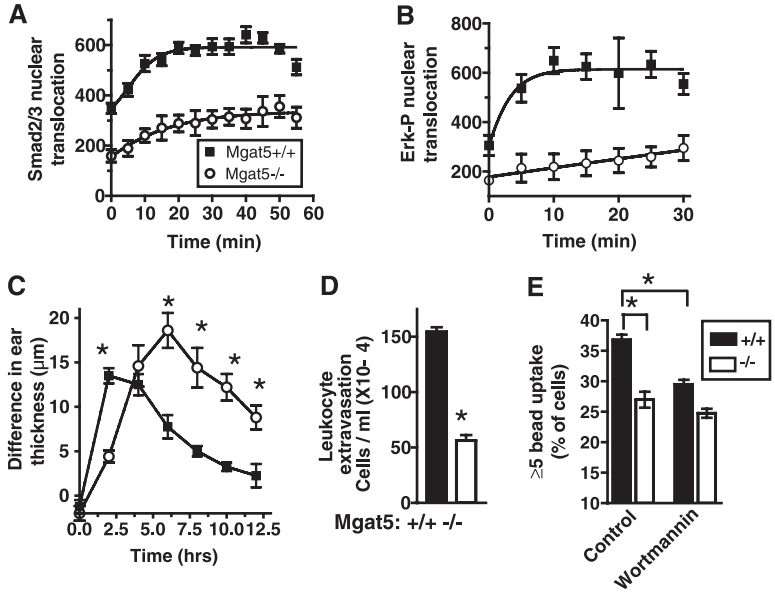

Fig. 4. Macrophage signaling, migration, and phagocytosis are dependent on Mgat5. (**A**) Smad2 and 3 and (**B**) Erk-P nuclear translocation in LPS-elicited peritoneal macrophages from Mgat5$^{+/+}$ and Mgat5$^{-/-}$ mice stimulated TGF-β1 (2 ng/ml) and 5% FCS, respectively. (**C**) Ear swelling induced by topical application of arachidonic acid in Mgat5$^{-/-}$ (○) and Mgat5$^{+/+}$ (+) mice (*$P < 0.001$). (**D**) Leukocytes recruitment into the peritoneal cavity 3 hours after an injection of thioglycolate (*$P < 0.001$). (**E**) Phagocytosis of five or more fluorescent latex beads by thioglycolate-elicited macrophages, either untreated or treated with wortmannin (100 nM) for 1 hour ex vivo during bead phagocytosis (*$P < 0.01$). Values are mean ± SE for five mice per genotype.

These observations suggest that a transformation-associated increase in membrane remodeling and endocytosis may require the lattice to protect receptors at the surface. We found that nontransformed Chinese hamster ovary (CHO) cells and the lectin-resistant cell lines Lec1 and Lec8 all displayed similar responses to TGF-β, suggesting the lattice was not required (fig. S7A). The Lec1 and Lec8 cell lines are deficient in Mgat1 and Golgi uridine 5′diphosphate–Gal transporter activity, respectively, and consequently depleted for poly-N-acetyllactosamine and presumably the lattice. However, when these cell lines were transformed with polyomavirus large T (designated CHOP), signaling was significantly greater in the wild-type cells compared to the transformed Lec mutants (fig. S7B). To explore this with other cell lines, we treated transformed and nontransformed cells with swainsonine, a Golgi α-mannosidase II inhibitor that blocks processing upstream of Mgat5. Swainsonine reduced TGF-β responsiveness in B16F10 murine melanoma cells and SW620 human colorectal cancer cells but not in nontransformed murine epithelial NMuMG cells (fig. S7, C to F).

The motile and highly endocytic phenotype of activated macrophages is similar in this regard to tumor cells and may require the lattice to retain surface cytokine receptors. We examined this possibility by using lipopolysaccharide (LPS)-elicited peritoneal macrophages and determined that endogenous phospho-Smad2 and -Erk2 and 3, as well as acute responses to TGF-β and serum, were suppressed in Mgat5$^{-/-}$ cells (Fig. 4, A and B). Furthermore, binding of ^{125}I-labeled TGF-β1 to surface receptors was reduced in Mgat5$^{-/-}$ macrophages, characteristic of the Mgat5-deficient phenotype observed in tumor cells (fig. S5F). Early in the injury response, cytokines stimulate leukocyte migration, and subsequently TGF-β attains amounts that suppress the inflammatory process (*24*). Consistent with this chronology, we observed that skin inflammation induced by either arachidonic acid or phorbol ester was delayed in both its onset and its resolution phases in Mgat5$^{-/-}$ mice (Fig. 4C). Similarly, the initial rate of leukocyte extravasation into the peritoneal cavity in response to an injection of thioglycollate was impaired in Mgat5$^{-/-}$ mice (Fig. 4D), demonstrating that Mgat5 regulates leukocytes motility. Phagocytosis of latex beads by Mgat5$^{-/-}$ macrophages was reduced. The PI3 kinase inhibitor wortmannin reduced phagocytosis in wild-type macrophages but did not suppress further in Mgat5$^{-/-}$ cells (Fig. 4E). Thus, the lattice promotes responsiveness to extracellular cytokines in this example of a nontransformed but endocytic cell type. Mgat5 modification of N-glycans on integrins and other adhesion receptors may also influence membrane remodeling and extracellular matrix assembly (*25*).

Lattice-dependent regulation of receptors occurs primarily at the cell surface, is dependent on Golgi enzyme activities and the number of N-glycans per receptor, and opposes receptor loss to endocytosis (fig. S1B). Receptor tyrosine kinases activate Rab5, a small GTPase required for endocytosis (*17*), thereby promoting receptor loss, whereas our results show that positive feedback from signaling to the Golgi pathway strengthens the lattice, thereby maintaining cytokine responsiveness. Lastly, we speculate that genetic and environmental factors that regulate the integrity of the lattice should influence the decline in surface cytokine receptors known to occur with aging (*26*, *27*) and thereby progenitor cell and tissue renewal.

References and Notes

1. E. Ioffe, P. Stanley, *Proc. Natl. Acad. Sci. U.S.A.* **91**, 728 (1994).
2. M. Metzler *et al.*, *EMBO J.* **13**, 2056 (1994).
3. Y. Wang *et al.*, *Glycobiology* **11**, 1051 (2001).
4. M. Granovsky *et al.*, *Nat. Med.* **6**, 306 (2000).
5. P. Nangia-Makker *et al.*, *Am. J. Pathol.* **156**, 899 (2000).
6. Y. Levy, D. Ronen, A. D. Bershadsky, Y. Zick, *J. Biol. Chem.* **278**, 14533 (2003).
7. H. C. Gong *et al.*, *Cancer Res.* **59**, 6239 (1999).
8. R. C. Hughes, *Biochim. Biophys. Acta* **1473**, 172 (1999).
9. J. Hirabayashi *et al.*, *Biochim. Biophys. Acta* **1572**, 232 (2002).
10. S. Yousefi *et al.*, *J. Biol. Chem.* **266**, 1772 (1991).
11. N. Ahmad *et al.*, *J. Biol. Chem.* **279**, 10841 (2003).
12. M. Demetriou, M. Granovsky, S. Quaggin, J. W. Dennis, *Nature* **409**, 733 (2001).
13. M. A. Webster *et al.*, *Mol. Cell. Biol.* **18**, 2344 (1998).
14. C. J. Stroop *et al.*, *Glycobiology* **10**, 901 (2000).
15. H. S. Wiley, S. Y. Shvartsman, D. A. Lauffenburger, *Trends Cell Biol.* **13**, 43 (2003).
16. T. C. Elleman *et al.*, *Biochem. J.* **347**, 771 (2000).
17. L. Lanzetti, A. Palamidessi, L. Areces, G. Scita, P. P. Di Fiore, *Nature* **429**, 309 (2004).
18. P. Soubeyran, K. Kowanetz, I. Szymkiewicz, W. Y. Langdon, I. Dikic, *Nature* **416**, 183 (2002).
19. G. M. Di Guglielmo, C. Le Roy, A. F. Goodfellow, J. L. Wrana, *Nature Cell Biol.* **5**, 410 (2003).
20. M. Oft, R. J. Akhurst, A. Balmain, *Nature Cell Biol.* **4**, 487 (2002).
21. L. Chen, W. Zhang, N. Fregien, M. Pierce, *Oncogene* **17**, 2087 (1998).
22. E. Miyoshi *et al.*, *J. Biol. Chem.* **270**, 6216 (1995).
23. F. Palacios, J. K. Schweitzer, R. L. Boshans, C. D'Souza-Schorey, *Nature Cell Biol.* **4**, 929 (2002).
24. M. J. Crowe, T. Doetschman, D. G. Greenhalgh, *J. Invest. Dermatol.* **115**, 3 (2000).
25. M. Demetriou, I. R. Nabi, M. Coppolino, S. Dedhar, J. W. Dennis, *J. Cell Biol.* **130**, 383 (1995).
26. S. C. Park, *Mech. Ageing Dev.* **123**, 917 (2002).
27. H. Shiraha, K. Gupta, K. Drabik, A. Wells, *J. Biol. Chem.* **275**, 19343 (2000).

28. This research was supported by grants from the Canadian Institute for Health Research (CIHR) and a U.S. Army Breast Cancer Research grant to J.W.D. and a CIHR studentship to E.P. The authors thank A. Raz for Gal-3 antibodies and J. Hudson and C. Swallow for helpful discussion.

Supporting Online Material

www.sciencemag.org/cgi/content/full/306/5693/120/DC1
Materials and Methods
SOM Text
Figs. S1 to S7
Table S1

29 June 2004; accepted 13 August 2004

Src Mediates a Switch from Microtubule- to Actin-Based Motility of Vaccinia Virus

Timothy P. Newsome, Niki Scaplehorn, Michael Way*

The cascade of events that leads to vaccinia-induced actin polymerization requires Src-dependent tyrosine phosphorylation of the viral membrane protein A36R. We found that a localized outside-in signaling cascade induced by the viral membrane protein B5R is required to potently activate Src and induce A36R phosphorylation at the plasma membrane. In addition, Src-mediated phosphorylation of A36R regulated the ability of virus particles to recruit and release conventional kinesin. Thus, Src activity regulates the transition between cytoplasmic microtubule transport and actin-based motility at the plasma membrane.

The microtubule cytoskeleton provides many viruses with an efficient way to reach their site of replication, as well as a means for newly assembled viruses to leave their unwilling host (*1*, *2*). In the case of vaccinia virus, recruitment of conventional kinesin by intracellular enveloped virus (IEV) particles results in their microtubule-dependent transport from perinuclear assembly sites to the cell periphery (*3*–*7*). Upon reaching the plasma membrane, vaccinia induces localized actin polymerization that acts to enhance cell-to-cell spread of the virus (*4*, *5*, *7*–*9*). Vaccinia actin tail formation, which occurs beneath the extracellular cell-associated enveloped virus (CEV) at the plasma membrane (*4*, *5*, *10*), appears to mimic receptor kinase signaling at the leading edge of motile cells (*11*–*14*). Src-dependent phosphorylation of Tyr^{112} and Tyr^{132} of A36R results in the generation of binding sites for the SH2 (Src homology 2) domains of the adapter proteins Nck and Grb2, respectively (*11*, *14*). Nck is recruited to the virus as a complex with WASP interacting protein (WIP) and N-WASP; this complex is stabilized by additional interactions with Grb2 (*11*, *12*, *14*–*16*). Ultimately, recruitment of N-WASP leads to stimulation of the actin-nucleating activity of the Arp2/3 complex and actin tail formation (*13*).

To address how the microtubule and actin phases of virus transport are coordinated at the plasma membrane, we examined the regulation of A36R phosphorylation, which is the most upstream event of actin tail formation. Src activity is required for actin tail formation (*11*), but it is not clear whether A36R is a Src substrate. In in vitro kinase assays using purified components, Src was able to phosphorylate Tyr^{112} of A36R (residues 24 to 118) directly, and this led to the binding of Nck (Fig. 1A) (*17*). Neither Src-mediated phosphorylation of A36R (residues 24 to 118) nor the subsequent binding of Nck disrupted its interaction with conventional kinesin in vitro (*18*) (Fig. 1A). Endogenous Src kinase was localized beneath CEV particles that were promoting actin polymerization. Src kinase recruited to CEV was also phosphorylated at Tyr^{418}, indicating the active conformation of the kinase (Fig. 1B). Activated Src was not detected on kinesin-positive IEV or in cells that lack Src (Figs. 1C and 2A) (*17*). To determine whether A36R phosphorylation was restricted to the plasma membrane in response to Src recruitment, we raised antibodies against a phosphopeptide corresponding to Tyr^{132} of A36R (anti–A36R-$Y132PO_4$) (*17*). Anti–A36R-$Y132PO_4$ detected a signal beneath actin tail–inducing CEV at the plasma membrane, but not on A36R-Y132F virus (Fig. 1, D and E). No signal was observed with anti–A36R-$Y132PO_4$ on kinesin-positive IEV in the cytoplasm (Fig. 2C). The pattern of A36R phosphorylation reflected a subset of the total distribution of A36R, which was also observed on the perinuclear trans-Golgi network as well as on IEV being transported to the plasma membrane on microtubules (Figs. 1D and 2C). The absence of a signal on kinesin-positive IEV suggests that Src-mediated phosphorylation of A36R occurred only when the virus reached the plasma membrane, and not before.

To confirm that Src recruitment and activation occur upstream of A36R phosphorylation, we looked for evidence of the presence of the kinase on A36R-YdF virus particles that cannot induce actin tails because Tyr^{112} and Tyr^{132} of A36R have been mutated to Phe (*5*). A36R-YdF virus particles recruited active Src, indicating that its activation was independent of interactions

Cell Motility Laboratory, Room 529, Cancer Research UK, London Research Institute, Lincoln's Inn Fields Laboratories, 44 Lincoln's Inn Fields, London WC2A 3PX, UK.

*To whom correspondence should be addressed. E-mail: michael.way@cancer.org.uk